Taylor & Francis
Taylor & Francis Group

Persistence and dynamics of fluorescent *Lactobacillus plantarum* in the healthy *versus* inflamed gut

Sophie Salomé-Desnoulez[a], Sabine Poiret[b], Benoit Foligné[c], Ghaffar Muharram[b], Véronique Peucelle[b], Frank Lafont[a,b], and Catherine Daniel[b]

[a]Univ. Lille, CNRS, INSERM, CHU Lille, Institut Pasteur de Lille, US 41 - UMS 2014 - PLBS, F-59000 Lille, France; [b]Univ. Lille, CNRS, INSERM, CHU Lille, Institut Pasteur de Lille, U1019 - UMR 9017 – Center for Infection and Immunity of Lille, F-59000 Lille, France; [c]Univ. Lille, INSERM, CHU Lille, U1286 - Infinite - Institute for Translational Research in Inflammation, F-59000 Lille, France

ABSTRACT

The gastrointestinal tract is the main ecological niche in which *Lactobacillus* strains may provide health benefits in mammals. There is currently a need to characterize host-microbe interactions in space and time by tracking these bacteria *in vivo*. We combined noninvasive whole-body imaging with *ex vivo* fluorescence confocal microscopy imaging to monitor the impact of intestinal inflammation on the persistence of orally administered *Lactobacillus plantarum* NCIMB8826 in healthy and inflamed mouse colons. We developed fluorescent *L. plantarum* strains and demonstrated that mCherry is the best system for *in vivo* imaging and *ex vivo* fluorescence confocal microscopy of these bacteria. We also used whole-body imaging to show that this anti-inflammatory, orally administered strain persists for longer and at higher counts in the inflamed colon than in the healthy colon. We confirmed these results by the *ex vivo* confocal imaging of colons from mice with experimental colitis for 3 days after induction. Moreover, extended orthogonal view projections enabled us to localize individual *L. plantarum* in sites that differed for healthy *versus* inflamed guts. In healthy colons, orally administered bacteria were localized in the lumen (in close contact with commensal bacteria) and sometimes in the crypts (albeit very rarely in contact with intestinal cells). The bacteria were observed within and outside the mucus layer. In contrast, *L. plantarum* bacteria in the inflamed colon were mostly located in the lumen and (in less inflamed areas) within the mucus layer. In more intensely inflamed areas (i.e., where the colon had undergone structural damage), the *L. plantarum* were in direct contact with damaged epithelial cells. Taken as a whole, our results show that fluorescently labeled *L. plantarum* can be used to study the persistence of these bacteria in inflamed guts using both noninvasive whole-body imaging and *ex vivo* fluorescence confocal microscopy.

Introduction

Lactobacillus plantarum NCIMB8826 (the parental strain of *L. plantarum* WCFS1 isolated from human saliva) is one of the most extensively studied *Lactobacillus*. For example, its genome was sequenced over 15 years ago (for a review, see[1]). The bacterium can be grown to high densities and can easily be transformed with genetic tools for the development of live mucosal delivery vectors [2]. *L. plantarum* NCIMB8826 has a "Qualified Presumption of Safety" (from the European Food Safety Authority) and "Generally Recognized as Safe" status (from the US Food and Drug Administration). It also has well-proven health benefits when administered to mice. Indeed, in a murine model of colitis induced by 2,4,6-trinitrobenzene sulfonic acid (TNBS), administration of this strain led to a dose-dependent protection in animals with slightly to moderately severe colitis.[3,4] Moreover, *L. plantarum* NCIMB8826 counters excessive immune responses in a murine model of birch pollen allergy[5] and alleviates metabolic disorders in mice fed a high-fat diet.[6] Lastly, a large number of molecular studies have focused on this strain.[7] Better knowledge of the bacterium has prompted suggestions that several other properties (such as effects on epithelial barrier function, stimulation of Th1 cells, and the potential to remove cholesterol) could be exploited further.[1]

L. plantarum NCIMB8826 is also very robust and has a relatively high survival rate for passage

through the human gastrointestinal tract (GIT); as such, it has become the "gold standard" *Lactobacillus* strain for studies of persistence in the GIT. For example, high densities (10^8 CFU g^{-1}) of live *L. plantarum* NCIMB8826 were found in human fecal samples after 7 days of consuming 150 g of fermented milk three times a day.[8] Another clinical study in healthy volunteers demonstrated that *L. plantarum* WCFS1 survived passage through the GIT, since levels of the bacterium in human fecal samples were 100 to 1000 times higher than those of other *L. plantarum* strains until 3–4 days after administration.[9] Moreover, we and others have shown that oral administration of *L. plantarum* WCFS1 or NCIMB8826 in a mouse model resulted in the persistence of the strain in the feces for at least 7 days.[10–12] Taken as a whole, these results demonstrate that *L. plantarum* NCIMB8826 is a very suitable model of spatiotemporal interactions between bacteria and the host's GIT.

The GIT is the main ecological niche for *Lactobacillus* strains, although distal effects outside the gut have been described.[13] When present in the murine or human GIT, some *Lactobacillus* strains show common characteristics that may be related to their adaptation to the intestinal niche.[14] The ability to directly track *in vivo* changes in space and time will help us to gain a better understanding of the lactobacilli's survival, metabolic activities, and interactions in the GIT. Using small animal *in vivo* bioluminescence imaging and the expression of distinct luciferases in *L. plantarum* NCIMB8826, we have studied the persistence and precise localization of these bacteria in the mouse GIT.[12,15] This noninvasive method provides key data on bacterial dissemination in the live animal.[16] An alternative to bioluminescence imaging is fluorescence imaging; the latter technique is less sensitive and has a lower signal-to-noise ratio but saves time and avoids the need to add luciferin as a substrate. Relative to bioluminescence imaging, fluorescence imaging also requires shorter exposure times. Several fluorescent proteins (including mCherry, infrared fluorescent proteins, and the monomeric blue protein mTagBFP2) have been expressed in other *Lactobacillus* strains, such as *L. plantarum* ATCC8014,[17] *L. plantarum* 423,[18] *Lactobacillus rhamnosus* GG,[19] and the *Lactobacillus reuteri* ATCC PTA6475 and R2LC strains.[18] However, very few studies have successfully tracked

these fluorescent bacteria in live mice. Indeed, the overlap with hemoglobin absorption and strong tissue autofluorescence limits detection of the fluorophores *in vivo*. Berlec *et al.* have already shown that orally administered *L. plantarum* ATCC8014 producing infrared fluorescent proteins can be tracked in live mice by *in vivo* fluorescence imaging.[17] Moreover, Karimi *et al.* were able to visualize *L. reuteri* ATCC PTA6475 and R2LC strains producing the mCherry fluorescent protein immediately after oral administration but not one hour later, when the signal became too weak.[20] Thus, there is currently a need to track *Lactobacillus* strains *in vivo* in space and time, in order to characterize host-microbial interactions potentially related to beneficial effects on health. We thus developed various recombinant *L. plantarum* NCIMB8826 strains producing either GFP, mCherry, or dual luciferase-mCherry proteins and then used *in vivo* live imaging in anesthetized mice to track the bacteria' persistence and viability in the GIT. Here, we demonstrate that mCherry is the best system for noninvasive whole-body *in vivo* imaging of these bacteria in the mouse GIT after oral administration. After having developed this mCherry tool, we combined it with *ex vivo* fluorescence confocal microscopy to study the interactions between orally administered *L. plantarum* and intestinal cells. To this end, we examined freshly collected mouse intestinal tissues *ex vivo*. We have therefore characterized *L. plantarum*'s behavior in healthy mice and in mice with intestinal inflammation (experimental colitis).

Results

In vitro production of luciferase and fluorescent proteins in L. plantarum

The bioluminescence and fluorescence signals produced *in vitro* by the various recombinant *L. plantarum* strains (*i.e.* Lp-CBRluc, Lp-mCherry, Lp-CBRluc/mCherry, and Lp-GFP) were quantified in bacterial cultures (2.5×10^{11} CFU/ml) (Figure 1). The bioluminescence signal emitted by Lp-CBRluc was nearly an order of magnitude more intense than that emitted by Lp-CBRluc/mCherry (mean values: 4.0×10^{10} and 6.6×10^9 photons/s, respectively, $p < .01$). Moreover, Lp-mCherry and Lp-GFP emitted more intense fluorescence signals than Lp-CBRluc/mCherry did, with mean values of 4.9
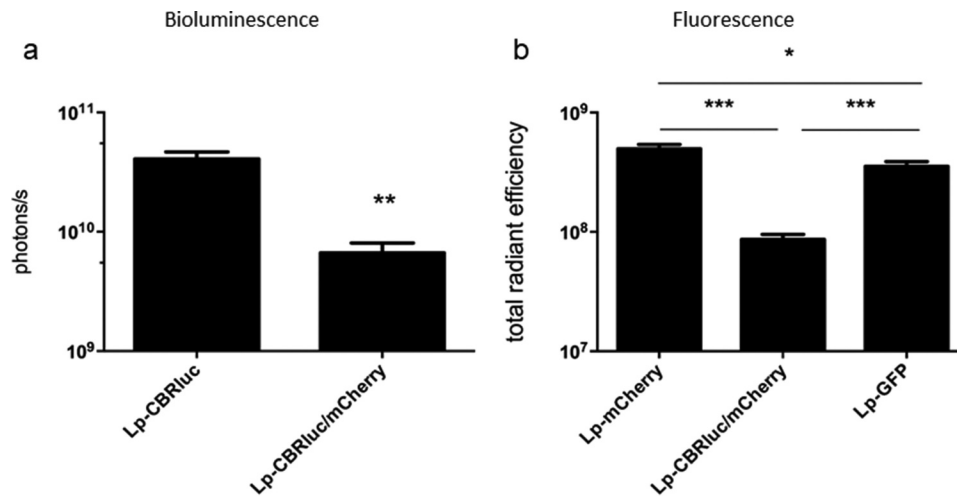
Bioluminescence

Fluorescence

Figure 1. *In vitro*, Lp-CBRluc and Lp-mCherry emitted the highest fluorescence signal and bioluminescence signal, respectively. Bioluminescence (a) was measured in cultures of Lp-CBRluc and Lp-CBRluc/mCherry, and fluorescence (b) was measured in cultures of Lp-mCherry, Lp-CBRluc/mCherry and Lp-GFP. Strains were cultured overnight (stationary phase). All strains were adjusted to 2.5×10^{11} CFU/ml and aliquoted into black microplates. The values shown are the means from three independent cultures, measured in triplicate. Results are given in p/s for bioluminescence and as the total radiance efficiency (in $[(p/s/cm^2/sr)/(\mu W/cm^2)]$) for fluorescence. The background for *L. plantarum*-pNZ8148 has been subtracted from each value. The error bars correspond to the standard deviation. Lp, *L. plantarum*. Overall differences between the groups were assessed using the Kruskal–Wallis nonparametric test: *p < .05, **p < .01, *** *p* < .001.

x 10^8, 3.5 x 10^8, and 8.6×10^7 photons s^{-1} cm^{-2} steradian^{-1} respectively (p < .001). Plasmids pMEC275, pMEC276, and pMEC289 in *L. plantarum* (corresponding to Lp-CBRluc, Lp-mCherry, and Lp-CBRluc/mCherry, respectively) were remarkably stable; all colonies were fully bioluminescent after approximately 100 generations (10 subcultures) in a nonselective medium.

Lp-mCherry emits the strongest signal in live mice after oral administration

The bioluminescence and fluorescence signals emitted by the various recombinant *L. plantarum* strains were quantified and compared in live mice after four daily oral administrations of a 5×10^{10} CFU dose of each strain. In three independent control experiments, oral administration of Lp-GFP did not give a detectable transcutaneous fluorescence signal. We could only detect an *ex vivo* signal on day 4 after dissection of the GIT (Fig. S1). We, therefore, decided to curtail our experiments with Lp-GFP and focus on the transcutaneous signals emitted in mice by Lp-CBRluc, Lp-CBRluc/mCherry and Lp-mCherry.

The three strains' respective bioluminescence and fluorescence signals were quantified daily by direct imaging in six anesthetized mice per group

(Fig. S2). Relative to LpCBRluc/mCherry, the bioluminescence signal obtained with Lp-CBRluc and the fluorescence signal obtained with Lp-mCherry were consistently stronger throughout the experiments. Bioluminescence detection was more sensitive than fluorescence detection because the latter's background signal was much stronger. In fact, the fluorescence signal was at the background level on day 6, whereas bioluminescence could still be detected on day 6 and only dropped to the background level on day 7 (as described previously[12]). However, given that our primary objective was to track *L. plantarum* in the mouse gut by combining *in vivo* whole-body imaging with *ex vivo* microscopy, Lp-mCherry was chosen for all further experiments because its fluorescence signals in live mice were much stronger than those of Lp-CBRluc /mCherry.

Lp-mCherry persists for longer in mice with experimental colitis than in healthy mice

We evaluated the impact of colon inflammation on the persistence of Lp-mCherry by comparing signals in healthy mice *versus* mice with experimental (TNBS-induced) colitis. Mice were given phosphate-buffered saline solution or a daily 5.0×10^9
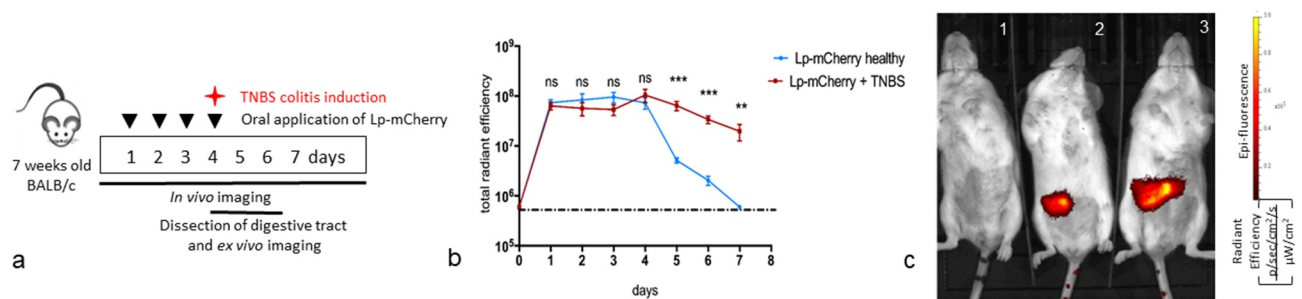
Figure 2. After four daily oral administrations in mice, *L. plantarum* persists for a longer in the inflamed colon than in the healthy colon. (a) The experimental design. Three groups of mice were constituted: (i) mice given Lp-mCherry for 4 days (5 x 10^9 CFU) prior to colitis induction (Lp-mCherry+TNBS), (ii) mice given Lp-mCherry for 4 days (5 x 10^9 CFU) without colitis induction (Lp-mCherry healthy) and (iii) negative control healthy mice given *L. plantarum* NCIMB8826 containing the empty vector pNZ8148. In the Lp-mCherry+TNBS group, colitis was induced on day 4 by the intrarectal administration of TNBS. Whole-body imaging was performed from day 1 to day 7. Mice were euthanized on days 4, 5 and 6, and the GITs were excised for *ex vivo* imaging. This experiment was repeated twice. (b) From day 0 to 7, the total radiant efficiency in [(p/s/cm^2/sr)/(μW/cm^2)] in whole animals for each set of six mice is shown, with its standard deviation. The background fluorescence is represented by a dashed line. Intergroup differences were assessed using the Kruskal Wallis nonparametric test. **p < .01, *** *p* < .001, ns: nonsignificant. (c) A representative image of three mice: (**1**) a nontreated control mouse, representing the background fluorescence, and (**2**)(**3**): two mice administered with given Lp-mCherry on day 4. Fluorescence emission between 575 and 650 nm was measured with a high-resolution filter after excitation at 460, 500 and 535 nm, resulting in the acquisition of several images. Live imaging software was then used to subtract the background fluorescence by spectral unmixing. The color bar indicates the radiant efficiency [(p/s/cm2/sr)/(μW/cm2)].

CFU dose of Lp-mCherry for four consecutive days (Figure 2(a)). In the control group, administration of TNBS induced colitis, substantial body weight loss, and colon inflammation within 2 days (Fig. S3). Oral pretreatment with Lp-mCherry was associated with a moderate but statistically significant degree of protection against TNBS outcomes, as judged by macroscopic lesions (mean Wallace score: 4; *p* < 0,05, Fig. S3b). Individual histological scores were not recorded for technical reasons; the same samples were used for *ex vivo* fluorescence and confocal microscopy imaging of the mouse colon. However, representative May–Grünwald-Giemsa-stained middle colon sections from another experiment are shown in Fig. S3d.

The fluorescence signal was quantified daily (using fluorescence imaging) in six anesthetized mice per group (Figure 2(b)). The signals in both groups were strong and did not differ significantly on day 1 or on the last day of oral administration (day 4). As expected, the signal from Lp-mCherry in healthy mice fell rapidly to background levels by day 7. In contrast, signals from mice with colitis remained significantly higher in all animals from day 0 to day 7. The signal decreased very slowly and was still significantly above background at the end of the experiment. We also investigated the persistence of Lp-mCherry and its fluorescence

signal in samples of feces (Fig. S4). For technical reasons, feces could not be collected from mice with colitis because they exhibited severe diarrhea. In healthy mice, the Lp-mCherry strain clearly persisted for 8 days after the last inoculation of bacteria (i.e., until day 12, Fig. S4b), as determined by bacterial counts and as described previously.[12] In contrast, the fluorescence signal in feces could only be detected for up to 2 days after the last inoculation (i.e., until day 6, Fig. S4c). In fact, the sensitivity of *in vivo* fluorescence imaging is limited by the number of bacteria. If this number falls below a certain limit (approximately 4.0 × 10^4 CFU/100 mg feces, in our experiments), the fluorescence signal can no longer be detected – despite the presence of bacteria in the GIT and thus in the feces. Plating the feces samples to monitor the bacterial load is more sensitive and so this variable was always measured in parallel during our experiments.[12] Complete removal of bacteria from the GIT was confirmed by fecal plating only. Although fecal plating and *in vivo* imaging are complementary techniques, only the latter technique could determine where in the GIT the bacteria were located.

Lastly, we can assert that the persistence of Lp-mCherry in healthy mice was not dose-dependent (Fig. S5): greater doses (5.0 x 10^{10} CFU) were associated with a higher concentration of bacteria in the

feces but the persistence was fairly similar. Indeed, the bacteria persisted in the feces until day 12 (8 days after the last oral administration) for the mice given Lp-mCherry at a daily dose of 5.0×10^8 CFU and 5.0×10^9 CFU and until day 13 (1-day difference) for the mice given Lp-mCherry 5.0×10^{10} CFU.

The behavior of Lp-mCherry differs in the healthy versus inflamed gut

To extend our whole-body-imaging studies of the persistence of *L. plantarum* in the murine GIT, we next characterized the strain's behavior in various intestinal compartments via *ex vivo* fluorescence and confocal microscopy of freshly collected tissues after four daily oral administrations (Figure 2(a)). All tissues for whole-body imaging (using the IVIS® Lumina imaging system) were collected from the same fasting mice after dissection. The proximal colon was immediately opened, stained, immobilized in low-melting-temperature agarose and observed by confocal microscopy within an hour of removal. The tissues were not fixed. Given that the TNBS-induced inflammation is restricted to the colon, the macroscopic appearance of the ileum and cecum was similar in TNBS mice and healthy

mice; hence, ileal and cecal samples were only dissected from healthy/control mice. This method allowed us to visualize the whole thickness of each compartment of the intestine, using deep (z plane) imaging. Furthermore, large expanses (x-y planes) of the opened mucosal surface could be captured in full z depth by tiling the acquired images.

On day 4 (the last day of oral administration of the strain), the *ex vivo* fluorescence signal was strong; *L. plantarum* was predominantly found in the cecum and the colon, as described previously[12] (Figure 3(a)). On day 4 (corresponding to the onset of colitis), the colon was not yet inflamed and so did not differ when comparing healthy and TNBS-treated mice. The confocal microscopy images also showed that large numbers of *L. plantarum* (in red, in the Figure) were present on large expanses of the mucosa of the proximal colon in healthy mice (10x objective; Figures 3b and 25x objective; Figure 3c). The zoomed three-dimensional (3D)-rendered image was prepared by thresholding the signals from the cell nuclei, mucus, and bacteria and then creating an iso-surface to better visualize the bacteria in contact with host cells. The representative image in Figure 3d
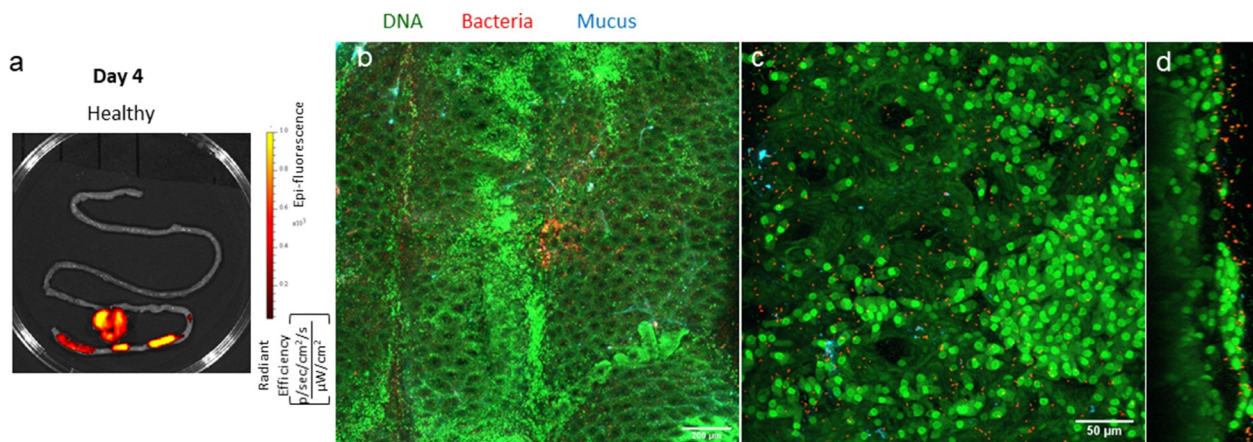

Figure 3. Using *ex vivo* fluorescence and confocal microscopy imaging, we found large numbers of *L. plantarum* in freshly collected colons on day 4 (i.e. after four daily oral administrations). Healthy mice and TNBS-treated mice were given Lp-mCherry (5 x 10^9 CFU, represented in red) for 4 days. Intestines (n = 4) were imaged *ex vivo* and the mouse colons were then stained with acriflavine (staining the nucleus in green) and wheat germ agglutinin Alexa Fluor 633 (in blue). On day 4, we induced colitis by administration of TNBS. Hence, at this time point, the colon was not yet inflamed and did not differ from the colon in healthy mice. This experiment was repeated three times. (a) A representative image of the fluorescence signal found in the GIT of a single healthy mouse. The color bar indicates the radiant efficiency [(p/s/cm²/sr)/(μW/cm²)]. (b, c) Confocal microscopy imaging, with representative 10x (**b**, scale: 200 μm) and 25x (**c**, scale: 50 μm) tiling images of the mouse colon. (d, h) A representative 3D-rendered image of the mouse colon.

shows that most of the bacteria were far from the intestinal cells; the only cells with proximal bacteria were senescent cells. We also observed that *L. plantarum* was present in large numbers in the murine cecum and ileum on day 4 (Figure S6).

On day 5, the *ex vivo* signal from Lp-mCherry in the GIT was hardly detectable in healthy mice but was intense in mice with colitis (similar parameters were used to quantify the radiant efficiency: Figure 4a and 4e). These results are in line with our whole-body imaging results for live animals (Figure 2b) and were also confirmed by our *ex vivo* confocal microscopy experiments (Figure 4). Indeed, only a few individual *L. plantarum* could be detected in healthy colons (as well as in healthy cecum and ileum: Figure

S6), whereas very high numbers were found in inflamed colons. The healthy proximal colon featured a continuous array of well-defined crypts with a macroscopically uniform appearance. In contrast, the inflamed colon (mean Wallace score: 4) featured large areas of necrotic, damaged tissue lacking any clear structure or crypts and just a few areas of healthy tissue with well-defined crypts. Moreover, extended orthogonal-view projections of the inflamed colon revealed large numbers of individual bacteria in direct contact with damaged cells (Figure 4h). In contrast, very few individual bacteria were still present in healthy colons. These distinct differences in *L. plantarum*'s presence and location between healthy and inflamed colons were also observed on day 6 (Figure 5).
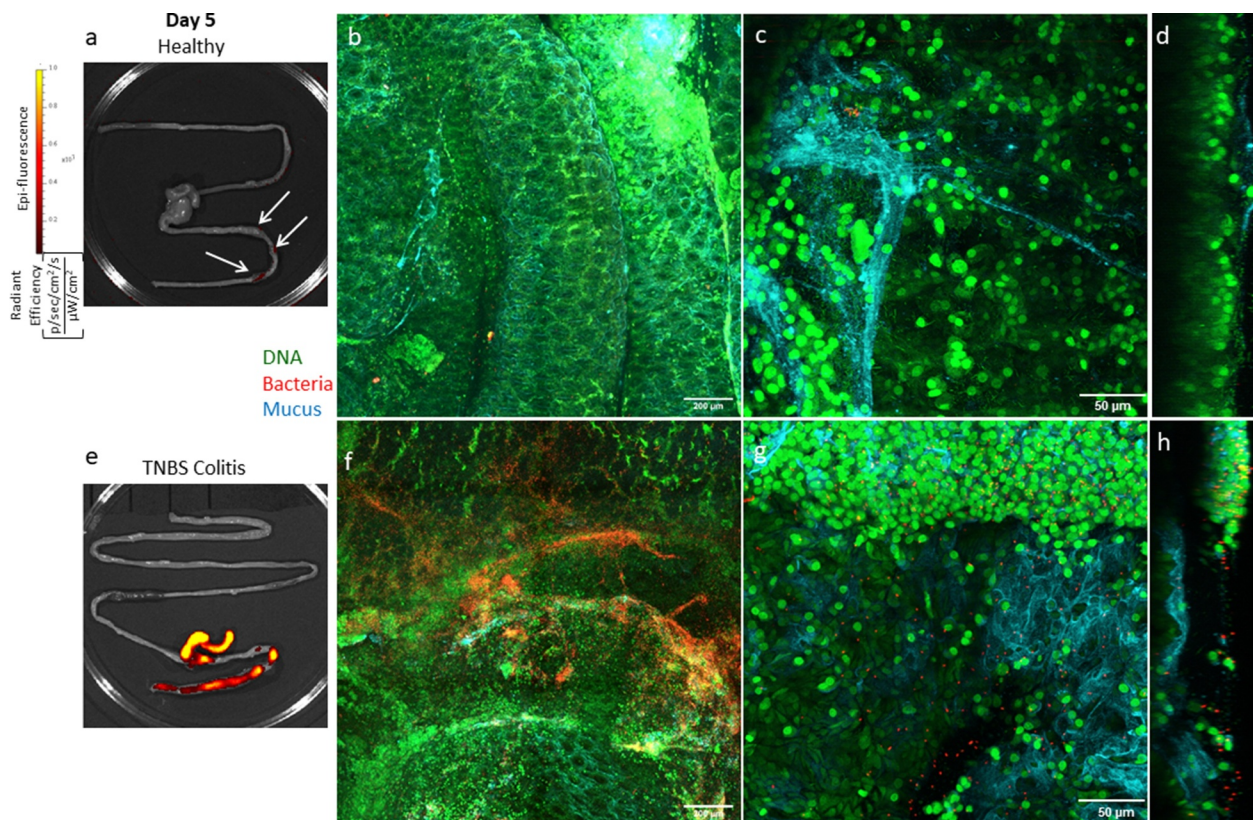

Figure 4. Using *ex vivo* fluorescence and confocal microscopy imaging, we found larger numbers of *L. plantarum* in freshly collected inflamed colons on day 5. Healthy and TNBS treated mice were given Lp-mCherry (5 x 10^9 CFU, in red) for 4 days. Intestines (n = 4) were imaged *ex vivo* and the mouse colons were then stained with acriflavine (staining the nucleus in green) and wheat germ agglutinin Alexa Fluor 633 (in blue). On day 4, we induced colitis by TNBS administration. This experiment was repeated three times. (a, e) Representative images of the fluorescence signal found in the GIT of one mouse per group (healthy mice and TNBS mice). The color bar indicates the radiant efficiency [(p/s/cm^2/sr)/(µW/cm^2)]. White arrows indicate weak fluorescence signals in healthy intestines. (b, c, f and g) Confocal microscopy imaging, with representative 10x (b, f, scale: 200 µm) and 25x (c, g, scale: 50 µm) tiling images of one mouse colon per group (healthy mice and TNBS mice). (d, h) Representative 3D-rendered images of one mouse colon per group. Colons of TNBS mice on day 5 show marked signs of tissue damage, relative to the normal appearance of the colon.
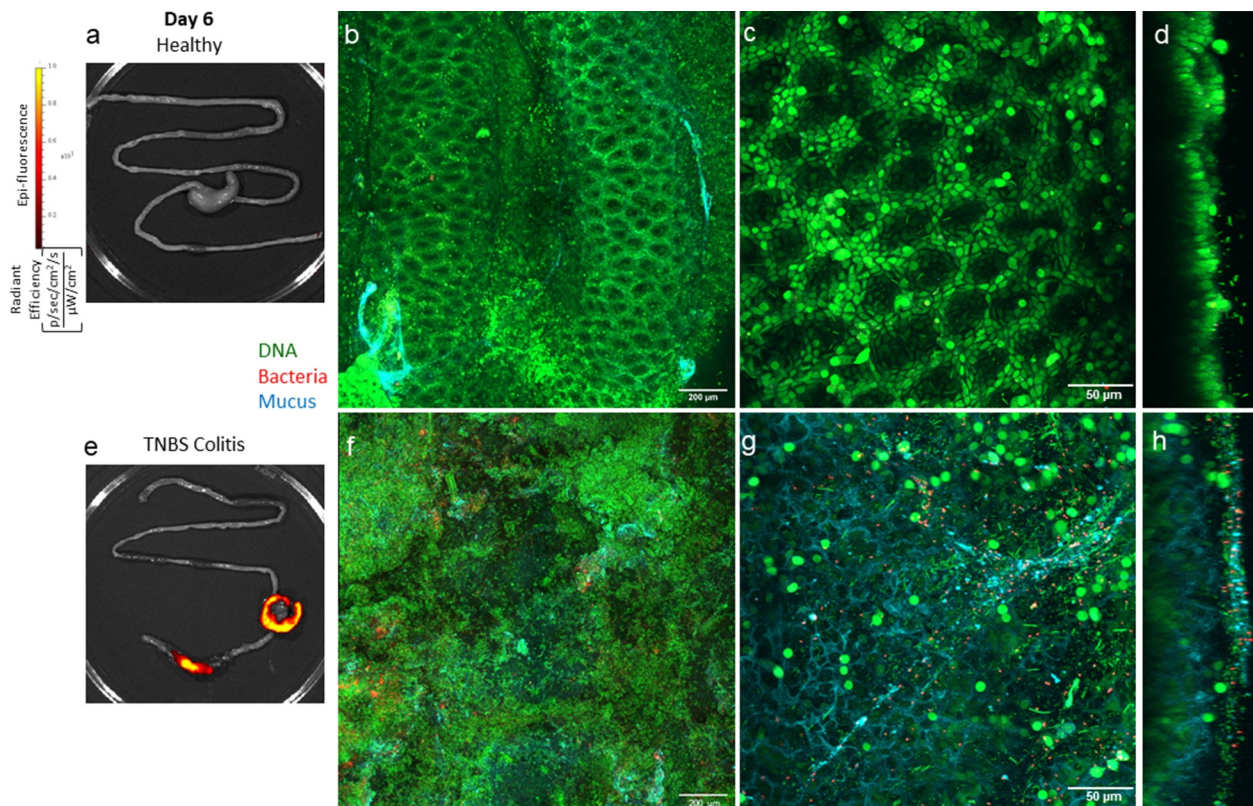
Figure 5. *L. plantarum* is found in higher amounts by *ex vivo* and confocal microscopy imaging in freshly collected inflamed colons on day 6. Healthy and TNBS treated mice were given Lp-mCherry (represented in red) for 4 days (5 x 10^9 CFU). Intestines (n = 4) were imaged *ex vivo* and the mouse colons were then stained with acriflavine (staining the nucleus in green) and wheat germ agglutinin Alexa Fluor 633 (in blue). On day 4, we induced colitis by TNBS administration. This experiment was repeated three times. (a, e) Representative images of the fluorescence signal found in the GIT of one mouse per group (healthy mice and TNBS mice). The color bar indicates the radiant efficiency [(p/s/cm^2/sr)/(μW/cm^2)]. (**b, c, f** and **g**) Confocal microscopy imaging, with representative 10x (**b, f** scale: 200 μm) and 25x (**c, g** scale: 50 μm) tiling images of one mouse colon per group (healthy mice and TNBS mice). (d, h) Representative 3D-rendered images of one mouse colon per group. Colons of TNBS mice on day 6 show marked signs of tissue damage, relative to the normal appearance of the healthy colon.

Direct contact between Lp-mCherry and intestinal cells is rare in the healthy colon and frequent in the inflamed colon

In order to precisely localize the bacteria within the intestine, we examined 3D-rendered images of healthy colons collected on day 4 (the day of the last oral administration) and inflamed colons collected on day 5 (Figure 6). As individual bacteria became difficult to find in healthy colons on day 5 (Fig. S7), we decided to evaluate the images from day 4. Various extended orthogonal view projections of healthy colons on day 4 enabled us to confirm the localization of the bacteria (in red) in the lumen and above and inside the crypts. The *L. plantarum* were in proximity to other endogenous bacteria in gut microbiota (cocci and bacilli, represented by green spots in the lumen) but were

rarely in direct contact with intestinal cells (Figure 6(a)). Moreover, *L. plantarum* was found both in the mucus layer and outside the mucus layer. Similar results were obtained in healthy ileums and colons (data not shown). In contrast, extended orthogonal view projections of inflamed colons on day 5 confirmed that large number of individual *L. plantarum* were present in the lumen and the mucus layer, where they were in direct contact with damaged or dead cells in inflamed areas of the colon lacking architecture (Figure 6(b)).

In order to precisely quantify the proximity of bacteria with colonic tissue, we quantified the proportion within 4 μm of a nucleus (in yellow in Figure S8). This value was approximately 3% in the healthy colon (154 out of 4250 individual spots on 12 different images of the proximal colon, cecum, and ileum
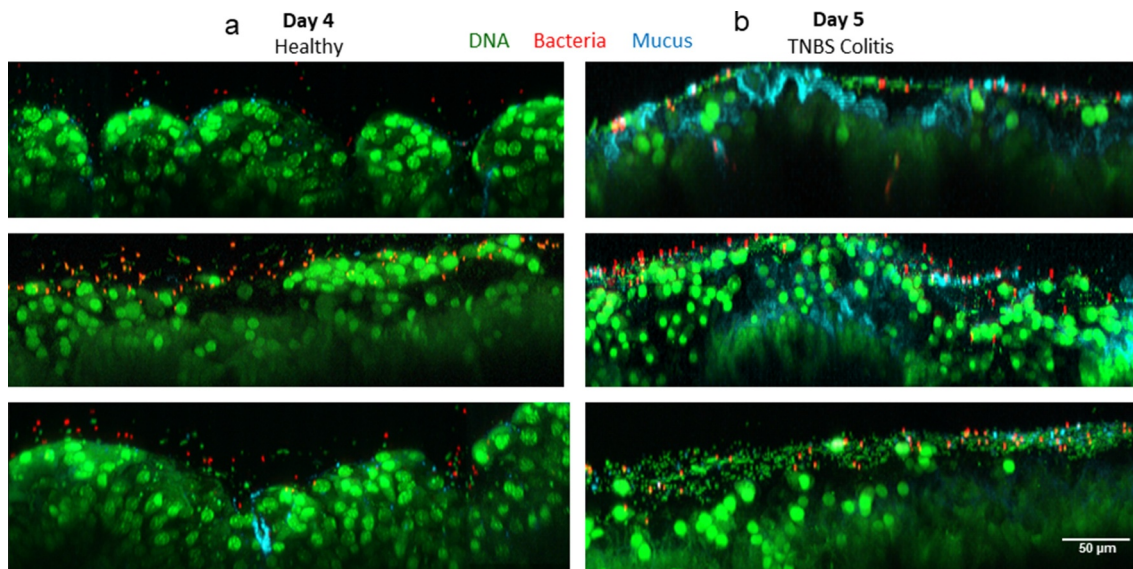
Figure 6. Direct contact between Lp-mCherry and intestinal cells is rare in the healthy colon, whereas bacteria are found in close proximity to the inflamed colonic tissue. Healthy and TNBS treated mice were given Lp-mCherry (5 x 10^9 CFU, in red) for 4 days. Mouse colons (n = 4/group) were imaged *ex vivo* and then stained with acriflavine (staining the nucleus in green) and wheat germ agglutinin Alexa Fluor 633 (in blue). On day 4, we induced colitis by TNBS administration. As individual bacteria became hard to observe in healthy colons on day 5, we decided to use the images from day 4 for healthy colons and from day 5 for inflamed colons. Representative 3D-rendered images of healthy colons (**a**, day 4) and inflamed colons (**b**, day 5) (three per group) are shown. Scale: 50 μm. The colons from TNBS mice on day 5 show marked signs of tissue damage, relative to the normal appearance of the healthy colon.

in three independent experiments). Thus, direct contact between bacteria and intestinal cells was a rare event – at least in the healthy colon. In fact, the bacteria in contact with the mucosal surface in the colon were close to senescent cells being eliminated during epithelial renewal.[21] In contrast to experiments in healthy mice, bacteria close to cell nuclei could not be quantified in inflamed colons because of the damaged tissue architecture.

Discussion

After producing two fluorescent proteins (the GFP superfolder and the mCherry in *L. plantarum* NCIMB8826) and a dual luciferase-mCherry recombinant protein, we showed that the mCherry system is the best for tracking orally administered bacteria in healthy mice via the whole-body *in vivo* imaging. This tool enabled us to assess the strain's persistence after ceasing oral administration; the bacteria were mainly found in the cecum and colon, as observed previously.[8] Although Karimi *et al.* built similar mCherry-producing *L. reuteri* strains (ATCC PTA6475 and R2LC), the whole-body *in vivo* imaging signals in

mice were detected for only a few minutes after a single administration.[20] Berlec *et al.* also reported the use of strains producing infrared fluorescent proteins to track *L. plantarum* and *Lactococcus lactis* after a single oral administration in mice. This system is attractive in theory because tissue autofluorescence in the mouse is minimal in the near-infrared region (between 700 and 1000 nm). However, the fluorescence signal could only be detected for 8 hours after a single administration. In contrast to the studies by Karimi *et al.* and Berlec *et al.*, we administered *L. plantarum* for 4 consecutive days; we had already shown that repeated administration increases the persistence of the strains in mice and gives a detectable fluorescence signal for a much longer period of time.[12] Moreover, we showed that the double luciferase-mCherry recombinant protein can be used to track the bacteria in mice. However, the bioluminescence and fluorescence signals were significantly less intense than in Lp-mCherry. Although Karimi *et al.* also engineered a double luciferase-mCherry recombinant protein in *L. reuteri*, the construct gave very low fluorescence and bioluminescence signals after a single oral administration in mice.[20]

As reported by others, we confirmed that *in vivo* bioluminescence imaging in mice is more sensitive and has a higher signal-to-noise ratio than fluorescence imaging – especially for red spectra with the added value of spectral unmixing algorithm.[22,23] However, fluorescence avoids time-consuming steps and the need to add luciferin substrate, and so we decided to use Lp-mCherry. The latter was best suited to tracking *L. plantarum* via a combination of small animal *in vivo* imaging and *ex vivo* confocal microscopic imaging.

In order to assess the behavior of *L. plantarum* in the healthy *versus* inflamed colon, we first used whole-body imaging to study the strain's persistence in healthy mice and in the TNBS experimental colitis model. The present study is the first to have shown that after oral administration in mice, *L. plantarum* (which provides a moderate degree of protection against colitis[3,24]) persists in larger numbers and for a longer period of time in the inflamed colon than in the healthy colon. This can be explained by the fact that *L. plantarum* mostly found in the mouse lumen and feces cannot be naturally expelled in damaged colons in mice having diarrhea. We then combined *ex vivo* imaging with confocal microscopy assessment of freshly collected healthy and inflamed intestinal tissues to localize *L. plantarum* on the single-cell scale. We imaged each sample within 30 minutes of removal, so that the spatial arrangement of the host tissue, mucus, and luminal contents (including microbes) was maintained as much as possible. However, we noticed that tissue degradation begins after 1 hour. A variety of novel tools and strategies have been developed to study the spatial organization of gut microbiota; most are based on immunofluorescence or *in situ* hybridization of fixed gut cross-sections in germ-free mice colonized with various labeled bacterial components of the murine or human microbiota.[25–27] However, it is important to note that fixing the gut tissue and preparing tissue sections modifies the native state of the mucus, due to the latter's high-water content. The widely used methacarn fixation method results in shrinkage of the mucus layer and the generation of mucus-free spaces adjacent to the epithelium.[28] The imaging approach applied in the present study maintains the host intestinal cells, digested material, commensal microbiota, exogenous bacteria, and mucus under near-native conditions. However, it should be noted that in dissected samples, (i) oxygen levels are higher than in the native gut, and (ii) peristalsis does not occur. In contrast to other researchers, we decided to use conventionally raised mice that already harbor microflora and thus constitute a more relevant physiological model than germ-free mice. Furthermore, germ-free mice have thinner mucus layers in the colon.[29,30] Thus, the transit and persistence of the administered strains may not be comparable.[25–27]

Our results showed that individual *L. plantarum* could be successfully imaged while transiting through the small intestine, cecum, proximal colon, and distal colon of healthy mice. These bacteria persisted in these intestinal compartments for 8 days after the last gavage. Using less sensitive small animal imaging techniques,[12] we did not find the persistence of *L. plantarum* in the small intestine (ileum). This might have been because *L. plantarum* is slightly less abundant in the small intestine than in the cecum and colon; the fluorescence or bioluminescence signal cannot be detected by whole-body or *ex vivo* imaging.

We used confocal imaging to confirm that the numbers of *L. plantarum* are significantly higher in freshly collected colons in the days after the induction of experimental colitis than in the corresponding samples from healthy mice. Moreover, extended orthogonal 3D projections enabled us to localize individual bacteria in different areas in healthy *versus* inflamed colons. In healthy colons, the bacteria were located often in the lumen (in close contact with other endogenous bacteria), sometimes in the crypts, and very rarely in contact with epithelial cells. *L. plantarum* was observed both in the mucus layer and outside the mucus layer. Our findings are in line with literature reports of the absence of commensal bacteria in direct contact with epithelial cells or the submucosa in the small intestine and colon of healthy mice.[31] This absence of direct contact can be explained by the presence of a physical (mucus) barrier, the thickness of which varies throughout the small intestine and the colon. In the colon, a thick firm layer of mucus overlays the epithelium and is devoid of bacteria – despite the large numbers of the latter residing in the lumen. In the small intestine, the mucus layer is thinner but bacteria are

rarely seen in contact with the epithelium – the exception being the intimate association between segmented filamentous bacteria and enterocytes in the mouse (for a review, see[28]). The architecture of the cecal mucus layer has only been partially described in a very recent study by Furter *et al.*; the mouse cecum was devoid of a continuous mucus layer.[32] This was surprising, since the microbiota is just as dense in the cecum as it is in the colon, and this mass of endogenous microbes should be in direct contact with the epithelium located between the crypts. However, Furter *et al.* did not study commensal bacteria.

In inflamed colons, most of the bacteria were (i) in the lumen and in the mucus layer in regions where the inflammation was less intense, and (ii) in direct contact with damaged epithelial cells in more intensely inflamed, destructured areas. The abnormal localization of commensal bacteria at the damaged colonic epithelium and the direct contact with host cells have been observed previously in murine colitis models other than the TNBS model[27,33] and in patients with ulcerative colitis.[33,34] In contrast to our present work, studies of commensal bacteria and non-orally-administered beneficial bacteria in murine colitis models or mucosal biopsies were all based on the analysis of fixed tissues.

Specific *Lactobacillus* and *Bifidobacterium* strains have been shown to exert beneficial properties in the inflamed gut[24,35,36] but their precise localization and behavior are not exactly known yet. Evaluating the survival and where bacterial interactions take place is essential to decipher the specific roles and mechanisms of such beneficial bacteria. Fluorescent probiotic *Lactobacillus* strains such as *L. reuteri* have been localized essentially in the cecum and colon of anesthetized mice by *in vivo* fluorescence imaging[20] whereas fluorescent *Bifidobacterium* strains have not been developed yet. We hypothesize that gut localization and behavior of *Lactobacillus* and *Bifidobacterium* strains might be different considering both the strain level and pathological conditions, i.e., during inflammation[37] as well as the corresponding altered microenvironment. Thus, our findings will enable us to study the distinct survival and properties of other probiotic strains as far as we are able to develop fluorescent candidate probiotics and

using the tools we developed for their *in vivo* detection. Moreover, we will be able to determine their interaction(s) with other microorganisms and host cells in the gut. This may also be helpful to study the localization of living probiotics provided in distinct matrices from fermented foods or designed with protective processes such as encapsulation.[38]

Given our observation of *L. plantarum*'s ability to protect the colon against colitis, we considered possible mechanisms of action based on its niche and its spatial behavior in healthy and inflamed guts. We found that a small proportion of *L. plantarum* persists in the healthy small intestine, colon, and cecum, where the strain might interact with the gut microbiota and the mucus layer but not directly with epithelial cells. We also showed that these bacteria persist in the gut for only a few days after the last administration; they are fully expelled in the feces approximately a week after the last gavage and do not durably colonize the gut, as already observed (Fig. S4).[12] In the inflamed gut, we speculate that the partially protective bacteria persist during inflammation and may interact with the gut microbiota, mucus, epithelial cells, and immune cells recruited to the inflamed region. In fact, *L. plantarum* WCSF1 (the bacterium used in the present study) has been shown to induce the expression of genes associated with anti-inflammatory activities in human duodenal biopsies from healthy adults a few hours after oral ingestion.[39] It has also been shown that perfusion of the human duodenum with this strain elicits structural changes in ZO-1 (zonula occludens 1/tight junction protein 1) and in transmembrane occludin complexes that are correlated with an enhanced barrier function.[40] Furthermore, *L. plantarum* NCIMB8826 interacts with the immune system; the strain has immunomodulatory effects on human dendritic cells and peripheral blood mononuclear cells *in vitro*.[3,41,42] These data illustrate the mechanisms by which *L. plantarum* WCSF1 may protect the gut against inflammation. However, these are still hypotheses because the studies in humans dealt with duodenal biopsies, and we did not study the mouse duodenum in detail. Given that direct contact between epithelial cells and the bacteria is very rare, one can also hypothesize that metabolites secreted by the bacteria protect the gut

against inflammation – as already described for other *Lactobacillus* strains.[43–45] Lastly, and given our observation of greater quantities of mucus and/or a thicker mucus layer in inflamed colons than in healthy colons, we speculate that *L. plantarum* NCIMB8826 increases the thickness of the mucus layer – as already observed and measured *in vivo* for *L. reuteri* strains in another mouse model of colitis.[35] Further, *in vivo* studies of these putative beneficial mechanisms are now warranted and could combine fluorescently labeled bacteria,[46–48] surface molecules from live bacteria (produced by metabolic engineering),[27] intravital microscopy of host-microbial interactions, and imaging-specific mediators of inflammation in real time.[49]

Material and methods

Bacterial strains, plasmids, and growth conditions

Bacterial strains and plasmids are listed in Table 1. The *L. plantarum* codon-optimized *mcherry* gene under the control of P*ldh*, the *L. plantarum* codon-optimized *superfolder gfp* gene under the control of P*ldh*, and the *L. plantarum* codon-optimized genes *cbrluc* and *mcherry* in fusion under the control of P*ldh* were cloned into pNZ8148 as *Bgl*II-*Xba* I fragments, respectively. These three DNA fragments were synthesized by Eurogentec, Liège, Belgium. The three resulting constructs were subsequently introduced into *L. plantarum* NCIMB8826 by electrotransformation, as described elsewhere[50] and named Lp-mCherry, Lp-GFP, and Lp-CBRluc/mCherry, respectively. *L. plantarum* NCIMB8826 containing the empty vector pNZ8148 (named *L. plantarum*-pNZ8148) served as a control in the *in vitro* and *in vivo* experiments. Recombinant strain stability was tested by standard methodology in our laboratory.[51]

Escherichia coli strains were cultured in Luria-Bertani broth at 37 °C. *L. plantarum* strains were grown at 37 °C in MRS medium (Difco, Becton Dickinson, Le Pont de Claix, France). Chloramphenicol (Sigma-Aldrich, St Quentin Fallavier, France) was added to culture media for bacterial selection when necessary, at a final concentration of 20 μg/mL for *E. coli* and 10 μg/mL for *L. plantarum* strains.

Table 1. Bacterial strains, plasmids and abbreviations for recombinant strains used in this study

Strain, plasmids or abbreviations for recombinant strains	Description[a]	Reference or source
Strains:		
Lactobacillus plantarum NCIMB8826	Originally isolated from human saliva	NCIMB
Escherichia coli MC1061	araD139 Δ(ara–leu)7696 lacX74 galV galK hsr–hsm rpsL	Invitrogen
Plasmids:		
pNZ8148	Cm[r], *L. lactis* pSH71 replicon	MoBiTech
pMEC256	pNZ8148 carrying CBRluc cDNA optimized for *L. plantarum* codon fused to the *L. plantarum* P*ldh* promoter (lactate dehydrogenase)	This study
pMEC275		This study
pMEC276		This study
pMEC289		[9]
Abbreviations for strains:	pNZ8148 carrying mCherry cDNA optimized for *L. plantarum* codon fused to the *L. plantarum* P*ldh* promoter	This study
Lp-CBRluc		This study
Lp-CBRluc/mCherry	pNZ8148 carrying superfolder GFP cDNA optimized for *L. plantarum* codon fused to the *L. plantarum* P*ldh* promoter	This study
Lp-mCherry		
Lp-GFP	pNZ8148 carrying the fusion of CBRluc cDNA optimized for *L. plantarum* codon, a ribosome binding site and mCherry cDNA optimized for *L. plantarum* codon. All these inserts are fused to the *L. plantarum* P*ldh* promoter	
	L. plantarum producing the CBRluc luciferase	
	L. plantarum producing the CBRluc as well as the mCherry fluorescent protein	
	L. plantarum producing the mCherry fluorescent protein	
	L. plantarum producing the superfolder GFP fluorescent protein	

Cm[r], resistance to chloramphenicol

In vitro bioluminescence and fluorescence measurements

The bioluminescence of Lp-CBRluc and Lp-CBRluc/mCherry was quantified as described previously.[9] Briefly, recombinant bacteria were grown overnight, harvested by centrifugation, and washed with phosphate-buffered saline (PBS). Fifty microliters of each culture, adjusted to approximately 2.5×10^{11} CFU/ml, was distributed in black microplates (Nunc, Thermo Fisher, NY, USA) and imaged after the addition of 50 μl of the Bright-Glo luciferase (Promega, Madison, WI, USA). Recombinant bacteria were prepared in a similar way for fluorescence detection without any addition of substrate. Fluorescence and luminescence

were measured at room temperature on the IVIS Lumina XR imaging system (Perkin Elmer, Alameda, CA, USA) using the Living Image software (Perkin Elmer). Strains were compared on the basis of the total flux of emitted light, expressed as photons per second (p/s) for bioluminescence and total radiance efficiency $[(p/s/cm^2/sr)/(\mu W/cm^2)]$ for fluorescence measured per 1.2 10^{10} CFU of each bacterial culture. Emission of fluorescence was measured with high-resolution filters with different excitation wavelengths (460, 500, and 535 nm) and emission wavelengths (between 575 and 650 nm) resulting in the acquisition of several images with an exposition time of 3 seconds (the use of the emission wavelengths was optimized to obtain the highest signals *in vitro*). The Living Image software was then used for generating spectrally unmixed images and quantification of each fluorescent signal after removal of the autofluorescence background. Each individual well was manually selected as a region of interest (ROI). *L. plantarum* NCIMB8826 containing the empty vector pNZ8148 was used to measure the background luminescence and fluorescence.

Animal experiments and ethics statements

BALB/c mice (female, 6 weeks of age) were purchased from Charles Rivers (L'Arbresle, France), and maintained in pathogen-free animal holding facilities. The animal experiments complied with French legislation (Government Act 87–848). All the studies were approved by the local investigation ethics review board (Nord-Pas-de-Calais CEEA N° 75, Lille, France) and the French government (agreement n° APAFIS#201,608,251,651,940). Bacterial strains were grown overnight (stationary phase), harvested by centrifugation, and washed with PBS. Mice received various amounts of bacteria administered by oral gavage in 200 µl buffer (0.2 M NaHCO3 buffer containing 1% glucose, pH 8).

In vivo persistence of L. plantarum in the GIT of mice

In the experiments described in Fig S1 and Fig S2, mice received 5.10^{10} CFU of live Lp-CBRluc, Lp-CBRluc/mCherry, Lp-mCherry, or Lp-GFP for four consecutive days. This physiological dose was administered to mice in order to obtain the highest signals emitted by the different strains for comparison.

Groups of mice then received a daily dose of 5.10^9 CFU of live Lp-mCherry for four consecutive days via the intragastric route in the experiments (as this strain displayed the best results in the preliminary experiments). Control mice received the *L. plantarum*-pNZ8148 negative control strain in the different experiments. Fecal samples were collected individually at different time points and mechanically homogenized in MRS medium at 100 mg of feces/ml. Dilutions were plated on to the selective media described above and incubated before enumeration. No chloramphenicol-resistant bacterium was detected in non-inoculated mice. Mice were sacrificed by cervical dislocation, and mouse digestive tracts (from the end of the stomach to rectum) were immediately excised for *ex vivo* imaging.

Induction of TNBS experimental colitis in mice

Trinitrobenzenesulfonic acid (TNBS) was used to chemically induce colitis in a mouse model of gut inflammation. TNBS induced acute colitis was implemented in 7-week-old female BALB/c mice. Three groups of mice were constituted for this study: (i) control mice (n = 12) without any treatment prior to colitis induction, (ii) mice administered with Lp-mCherry for 4 days (5.10^9 CFU) prior to colitis induction (n = 15), and (iii) healthy mice without any treatment (n = 3). At day 4, colitis was triggered by the intrarectal administration of 50 µl TNBS (100 mg.kg^{-1}) in 0.9% NaCl/ethanol (50/50 v/v) in mice groups (i) and (ii) 4 hours after the last oral administration of strains. One or 2 days after the induction of colitis, mice were euthanized and mouse digestive tracts (from the end of the stomach to rectum) were immediately excised for *ex vivo* imaging, colon inflammation scoring, and microscopic colon imaging (as described in Fluorescence microscopy). Mice were weighed prior to TNBS administration and at sacrifice. After dissection, two independent observers blindly scored the macroscopic inflammation of the colon by using the Wallace score.[52] The Wallace score rates macroscopic lesions on a scale from 0 to 8 based on features reflecting inflammation, such as

hyperemia (score 1 to 2), moderate to intense thickening of the bowel (score 2 to 3), and the gradual extent of 1 cm-long ulceration (score 3 to 8), according to the maximal mouse colon length. Two-cm-long fragments of the distal colon were collected and frozen at – 80 °C for histological analysis: paraffin-embedded 5-µm sections stained with May–Grünwald–Giemsa were examined under the microscope and tissue lesions were scored according to the Ameho criteria.[53]

In vivo bioluminescence and fluorescence imaging

Bioluminescence and fluorescence imaging were performed using a multimodal IVIS Lumina XR imaging system (Perkin Elmer). Prior to imaging, mice were anesthetized with 2% isoflurane, as described previously.[7] D-luciferin potassium salt (Perkin Elmer) at 30 mg/ml was administered orally to animals 15 minutes before the oral inoculation of the recombinant CBRluc expressing strains (100 µl/mouse). Two hours later, all mice were placed into the specimen chamber of the IVIS imaging system where a controlled flow of 1.5% isoflurane in air was administered through a nose cone via a gas anesthesia system (Tem Sega, Lormont, France). Emission of luminescence was measured as described previously.[7] Emission of fluorescence was measured with high-resolution filters with different excitation wavelengths (500, 535, 570, 605, and 640 nm) and emission wavelengths (between 695 and 770 nm) resulting in the acquisition of several images with an exposition time of 3 seconds (the use of the emission wavelengths were optimized to obtain the highest signals in whole-body mouse imaging). The Living Image software was then used for generating spectrally unmixed images and quantification of each fluorescent signal. Fluorescence and bioluminescence were quantified using the Living Image software (given as the radiance efficiency in photons s^{-1} cm^{-2} steradian^{-1} per µW cm^{-2} and p/s, respectively). For anatomical localization, a pseudocolor image representing detected light intensity was generated using the Living Image software and superimposed over the gray scale reference photography. For each individual mouse, there was only ROI corresponding to the mouse digestive tract and this ROI was manually selected.

Statistical analysis

All analyses were performed by comparing experimental groups to their respective controls using the non-parametric one-way analysis of variance Mann–Whitney U-testing or by the two-tailed Student-t testing where appropriate (GraphPad Prism 6.0, California, USA). Data are presented as means ± SEM. Differences were judged to be statistically significant when the p-value was <0.05. However, p-values between 0.05 and 0.1 are specified to indicate trends.

Fluorescence microscopy: sample preparation, confocal microscopy, and image analysis

Healthy mice were administered with Lp-mCherry for four consecutive days (day 1 to day 4) as described previously and observed for imaging at days 4, 5, and 6 after fasting for 6 hours. Moreover, another group of mice was treated similarly and a TNBS colitis was induced on the last administration day (day 4) and observed at days 4, 5, and 6 after fasting for 6 hours. The healthy and inflamed mouse colon, healthy cecum, and healthy ileum (each 1.5 cm long and at the same spot in each mouse) were opened longitudinally, stained with 1 mg/ml of acriflavine (Sigma-Aldrich), as well as 5 µg/ml of wheat germ agglutinin Alexa Fluor 633 (Thermo Fisher, Eugene, OR, USA) for 15 minutes and rinsed in PBS for 1 min. Each sample was placed flat in a Petri dish with the inside facing up and immobilized in low melting agarose 1.5%. The samples were then observed within 30 minutes of removal. Imaging was performed using an upright line-scanning microscope system equipped with a resonant scanner and hybrid detector (confocal TCS SP8, Leica microsystems, Wetzlar, Germany). The microscope was fitted with several dry and water-immersion objectives having a high numeric aperture and long working distances, as required for imaging in-depth and tiled images (HC FluoTar L 25x/0.95 W, HCX PL FluoTAR 10x/0.30 PH1 objective, Leica microsystems). The number of images in a stack or the depth of imaging is determined by the topography and the penetration of light into the tissue. Pinhole size was set to 1 Airy unit. Tiled images were acquired with an overlap of 10% and a z spacing of 10 µm and

2 μm for the 10x and 25x objectives, respectively. The observed zone in the case of the mice group induced with TNBS colitis is a border zone between necrotic tissue and inflamed tissue. We have shown representative images in our manuscript from three independent experiments with approximately 30 mice total.

Tiled images 10x were cropped to 0.16 × 0.16 cm to visualize tissue features more easily, and 450x450μm regions were observed to accurately visualize the location of bacteria on the surface of the tissue. The image contrast was enhanced by deconvolution (AutoQuant, Media Cybernetics, Maryland, USA) and normalized for improved quantification of objects and print viewing. In Fig. 3, 4, 5 and S5, 10x and 25x image stacks were reduced to a two-dimensional maximum intensity Z-projection image (Fiji/ImageJ, https://imagej.nih.gov/). To localize the bacteria in the thickness of the stack, the extended orthogonal view projection and 3D montages were produced using Imaris9.3.1 software (Bitplane, Oxford Instruments, Zurich, Switzerland) (Figs 5 and 6).

Using 25x lens, images were collected in four different fields per sample in which bacteria are detected, from at least three independent experiments. For healthy mice, the total number of bacteria was calculated using the Imaris Spot detector function. The cell surface was estimated at 3 μm of the volume defined from the nucleus of the cell tissue. The number of bacteria in contact with the tissue was defined using the MatLab function "Find spot close to surface". This XTension found the subset of spots that were closer to the surface than the user-specified threshold. In our case, a bacterium was considered in contact with the tissue, if the distance between the center of the bacteria and the surface of the nucleus was less than 4 μm.

Author contributions

SS, SP, and CD designed, performed, and interpreted most of the experiments and prepared the manuscript. VP performed the experiments. SP built the bacterial strains, and SS, CD, and VP managed the animal experiments. BF, FL, and GM helped to draft and edit the manuscript and provided conceptual advice. All authors approved the final manuscript for submission.

Disclosure of interest

All the authors declared that they have no conflicts of interest.

Disclosure statement

No potential conflict of interest was reported by the authors.

References

1. Van Den Nieuwboer M, Van Hemert S, Claassen E, De Vos WM. Lactobacillus plantarum WCFS1 and its host interaction: a dozen years after the genome. Microb Biotechnol. 2016;9(4):452–465. 10.1111/1751-7915.12368.
2. Daniel C, Roussel Y, Kleerebezem M, Pot B. Recombinant lactic acid bacteria as mucosal biotherapeutic agents. Trends Biotechnol. 2011;29(10):499–508. 10.1016/j.tibtech.2011.05.002.
3. Foligne B, Nutten S, Grangette C. Correlation between in vitro and in vivo immunomodulatory properties of lactic acid bacteria. World J Gastroenterol. 2007;13(2):236–243. 10.3748/wjg.v13.i2.236.
4. Yin X, Heeney D, Srisengfa Y. Bacteriocin biosynthesis contributes to the anti-inflammatory capacities of probiotic lactobacillus plantarum. Benef Microbes. 2018;9(2):333–344. 10.3920/BM2017.0096.
5. Repa A, Grangette C, Daniel C. Mucosal co-application of lactic acid bacteria and allergen induces counter-regulatory immune responses in a murine model of birch pollen allergy. Vaccine. 2003;22(1):87–95. 10.1016/S0264-410X(03)00528-0.

6. Martinic A, Barouei J, Bendiks Z. Supplementation of lactobacillus plantarum improves markers of metabolic dysfunction induced by a high fat diet. J Proteome Res. 2018;17(8):2790–2802. 10.1021/acs.jproteome.8b00282.

7. Douillard FP, De Vos WM. Functional genomics of lactic acid bacteria: from food to health. Microb Cell Factories. 2014;13(Suppl 1):S8. 10.1186/1475-2859-13-S1-S8.

8. Vesa T, Pochart P, Marteau P. Pharmacokinetics of lactobacillus plantarum NCIMB 8826, lactobacillus fermentum KLD, and lactococcus lactis MG 1363 in the human gastrointestinal tract. Aliment Pharmacol Ther. 2000;14(6):823–828. 10.1046/j.1365-2036.2000.00763.x.

9. Van Bokhorst-van De Veen H, Van Swam I, Wels M, Pa B, Kleerebezem M. Congruent strain specific intestinal persistence of lactobacillus plantarum in an intestine-mimicking in vitro system and in human volunteers. PloS One. 2012;7(9):e44588. 10.1371/journal.pone.0044588.

10. Grangette C, Muller-Alouf H, Geoffroy M. Protection against tetanus toxin after intragastric administration of two recombinant lactic acid bacteria: impact of strain viability and in vivo persistence. Vaccine. 2002;20(27–28):3304–3309. 10.1016/S0264-410X(02)00301-8.

11. Van Bokhorst-van De Veen H, Mj S, Wels M. Genotypic adaptations associated with prolonged persistence of lactobacillus plantarum in the murine digestive tract. Biotechnol J. 2013;8(8):895–904. 10.1002/biot.201200259.

12. Daniel C, Poiret S, Dennin V, Boutillier D, Pot B. Bioluminescence imaging study of spatial and temporal persistence of lactobacillus plantarum and lactococcus lactis in living mice. Appl Environ Microbiol. 2013;79 (4):1086–1094. 10.1128/AEM.03221-12.

13. George F, Daniel C, Thomas M. Occurrence and dynamism of Lactic Acid bacteria in distinct ecological niches: a multifaceted functional health perspective. Front Microbiol. 2018;9:2899. 10.3389/fmicb.2018.02899.

14. Bron PA, Van Baarlen P, Kleerebezem M. Emerging molecular insights into the interaction between probiotics and the host intestinal mucosa. Nat Rev Microbiol. 2011;10(1):66–78. 10.1038/nrmicro2690.

15. Daniel C, Poiret S, Dennin V. Dual-color bioluminescence imaging for simultaneous monitoring of the intestinal persistence of lactobacillus plantarum and lactococcus lactis in living mice. Appl Env Microbiol. 2015;81(16):5344–5349. 10.1128/AEM.01042-15.

16. Van Zyl WF, Deane SM, Dicks LMT. In vivo bioluminescence imaging of the spatial and temporal colonization of lactobacillus plantarum 423 and enterococcus mundtii ST4SA in the intestinal tract of mice. BMC Microbiol. 2018;18(1):171. 10.1186/s12866-018-1315-4.

17. Berlec A, Zavrsnik J, Butinar M, Turk B, Strukelj B. In vivo imaging of lactococcus lactis, lactobacillus plantarum and Escherichia coli expressing infrared fluorescent protein in mice. Microb Cell Fact. 2015;14(1):181. 10.1186/s12934-015-0376-4.

18. Van Zyl WF, Deane SM, Dicks LMT. Use of the mCherry fluorescent protein to study intestinal colonization by enterococcus mundtii ST4SA and lactobacillus plantarum 423 in mice. Appl Environ Microbiol. 2015;81(17):5993–6002. 10.1128/AEM.01247-15.

19. Spacova I, Lievens E, Verhoeven T. Expression of fluorescent proteins in lactobacillus rhamnosus to study host-microbe and microbe-microbe interactions. Microb Biotechnol. 2018;11(2):317–331. 10.1111/1751-7915.12872.

20. Karimi S, Ahl D, Vagesjo E. In vivo and in vitro detection of luminescent and fluorescent lactobacillus reuteri and application of red fluorescent mCherry for assessing plasmid persistence. PLoS One. 2016;11(3): e0151969. 10.1371/journal.pone.0151969.

21. Skoczek DA, Walczysko P, Horn N. Luminal microbes promote monocyte-stem cell interactions across a healthy colonic epithelium. J Immunol Baltim Md 1950. 2014;193:439–451.

22. Cool SK, Breyne K, Meyer E, De Smedt SC, Sanders NN. Comparison of in vivo optical systems for bioluminescence and fluorescence imaging. J Fluoresc. 2013;23 (5):909–920. 10.1007/s10895-013-1215-9.

23. Qin C, Zhu S, Tian J. New optical molecular imaging systems. Curr Pharm Biotechnol. 2010;11(6):620–627. 10.2174/138920110792246519.

24. Foligné B, Nutten S, Steidler L. Recommendations for improved use of the murine TNBS-induced colitis model in evaluating anti-inflammatory properties of lactic acid bacteria: technical and microbiological aspects. Dig Dis Sci. 2006;51(2):390–400. 10.1007/s10620-006-3143-x.

25. Mark Welch JL, Hasegawa Y, McNulty NP, Gordon JI, Borisy GG. Spatial organization of a model 15-member human gut microbiota established in gnotobiotic mice. Proc Natl Acad Sci U S A. 2017;114(43):E9105–E9114. 10.1073/pnas.1711596114.

26. Earle KA, Billings G, Sigal M. Quantitative imaging of gut microbiota spatial organization. Cell Host Microbe. 2015;18(4):478–488. 10.1016/j.chom.2015.09.002.

27. Hudak JE, Alvarez D, Skelly A, Von Andrian UH, Kasper DL. Illuminating vital surface molecules of symbionts in health and disease. Nat Microbiol. 2017;2:17099. 10.1038/nmicrobiol.2017.99.

28. Tropini C, Earle KA, Huang KC, Sonnenburg JL. The gut microbiome: connecting spatial organization to function. Cell Host Microbe. 2017;21(4):433–442. 10.1016/j.chom.2017.03.010.

29. Hansson GC, Johansson ME. The inner of the two Muc2 mucin-dependent mucus layers in colon is devoid of bacteria. Gut Microbes. 2010;1(1):51–54. 10.4161/gmic.1.1.10470.

30. Schroeder BO. Fight them or feed them: how the intestinal mucus layer manages the gut microbiota. Gastroenterol Rep. 2019;7(1):3–12. 10.1093/gastro/goy052.

31. Swidsinski A, Sydora BC, Doerffel Y. Viscosity gradient within the mucus layer determines the mucosal barrier function and the spatial organization of the intestinal microbiota. Inflamm Bowel Dis. 2007;13(8):963–970. 10.1002/ibd.20163.

32. Furter M, Me S, Gc H, W-d H. Mucus architecture and near-surface swimming affect distinct salmonella typhimurium infection patterns along the murine intestinal tract. Cell Rep. 2019;27(9):2665–2678.e3. 10.1016/j.celrep.2019.04.106.

33. Johansson MEV, Gustafsson JK, Holmén-Larsson J. Bacteria penetrate the normally impenetrable inner colon mucus layer in both murine colitis models and patients with ulcerative colitis. Gut. 2014;63 (2):281–291. 10.1136/gutjnl-2012-303207.

34. Swidsinski A, Loening-Baucke V, Theissig F. Comparative study of the intestinal mucus barrier in normal and inflamed colon. Gut. 2007;56(3):343–350. 10.1136/gut.2006.098160.

35. Ahl D, Liu H, Schreiber O. Lactobacillus reuteri increases mucus thickness and ameliorates dextran sulphate sodium-induced colitis in mice. Acta Physiol Oxf Engl. 2016;217(4):300–310. 10.1111/apha.12695.

36. Martín R, Chain F, Miquel S. Using murine colitis models to analyze probiotics-host interactions. FEMS Microbiol Rev. 2017;41(Supp_1):S49–S70. 10.1093/femsre/fux035.

37. Duranti S, Longhi G, Ventura M, Van Sinderen D, Turroni F. Exploring the ecology of bifidobacteria and their genetic adaptation to the mammalian gut. Microorganisms. 2020;9(1). 10.3390/microorganisms 9010008.

38. Chua JCL, Hale JDF, Silcock P, Bremer PJ. Bacterial survival and adhesion for formulating new oral probiotic foods. Crit Rev Food Sci Nutr. 2020;60 (17):2926–2937. 10.1080/10408398.2019.1669528.

39. Van Baarlen P, Troost FJ, Van Hemert S. Differential NF-kappaB pathways induction by lactobacillus plantarum in the duodenum of healthy humans correlating with immune tolerance. Proc Natl Acad Sci U S A. 2009;106(7):2371–2376. 10.1073/pnas.0809919106.

40. Karczewski J, Troost FJ, Konings I. Regulation of human epithelial tight junction proteins by lactobacillus plantarum in vivo and protective effects on the epithelial barrier. Am J Physiol Gastrointest Liver Physiol. 2010;298(6):G851–859. 10.1152/ajpgi.00327.2009.

41. Meijerink M, Van Hemert S, Taverne N. Identification of genetic loci in lactobacillus plantarum that modulate the immune response of dendritic cells using comparative genome hybridization. PloS One. 2010;5(5):e10632. 10.1371/journal.pone.0010632.

42. Van Hemert S, Meijerink M, Molenaar D. Identification of lactobacillus plantarum genes modulating the cytokine response of human peripheral blood mononuclear cells. BMC Microbiol. 2010;10(1):293. 10.1186/1471-2180-10-293.

43. Yan F, Cao H, Cover TL. Colon-specific delivery of a probiotic-derived soluble protein ameliorates intestinal inflammation in mice through an EGFR-dependent mechanism. J Clin Invest. 2011;121(6):2242–2253. 10.1172/JCI44031.

44. Bron PA, Kleerebezem M, Brummer R-J. Can probiotics modulate human disease by impacting intestinal barrier function?. Br J Nutr. 2017;117(1):93–107. 10.1017/S0007114516004037.

45. Liu Q, Yu Z, Tian F. Surface components and metabolites of probiotics for regulation of intestinal epithelial barrier. Microb Cell Factories. 2020;19(1):23. 10.1186/s12934-020-1289-4.

46. Geva-Zatorsky N, Alvarez D, Hudak JE. In vivo imaging and tracking of host-microbiota interactions via metabolic labeling of gut anaerobic bacteria. Nat Med. 2015;21(9):1091–1100. 10.1038/nm.3929.

47. Whitaker WR, Shepherd ES, Sonnenburg JL. Tunable expression tools enable single-cell strain distinction in the gut microbiome. Cell. 2017;169(3):538–546.e12. 10.1016/j.cell.2017.03.041.

48. Wang W, Zhang N, Du Y. Three-dimensional quantitative Imaging of native microbiota distribution in the gut. Angew Chem Int Ed Engl. 2020;60(6):3055–3061.

49. Dmochowska N, Wardill HR, Hughes PA. Advances in imaging specific mediators of inflammatory bowel disease. Int J Mol Sci. 2018;19(9). 10.3390/ijms19092471.

50. Wells JM, Wilson PW, Le Page RW. Improved cloning vectors and transformation procedure for lactococcus lactis. J Appl Bacteriol. 1993;74(6):629–636. 10.1111/j.1365-2672.1993.tb05195.x.

51. Pavan S, Hols P, Delcour J. Adaptation of the nisin-controlled expression system in lactobacillus plantarum: a tool to study in vivo biological effects. Appl Env Microbiol. 2000;66(10):4427–4432. 10.1128/AEM.66.10.4427-4432.2000.

52. Wallace JL, MacNaughton WK, Morris GP, Beck PL. Inhibition of leukotriene synthesis markedly accelerates healing in a rat model of inflammatory bowel disease. Gastroenterology. 1989;96(1):29–36. 10.1016/0016-5085(89)90760-9.

53. Ameho CK, Adjei AA, Harrison EK. Prophylactic effect of dietary glutamine supplementation on interleukin 8 and tumour necrosis factor alpha production in trinitrobenzene sulphonic acid induced colitis. Gut. 1997;41 (4):487–493. 10.1136/gut.41.4.487.